We like to thank the anonymous reviewer for the comments which helped improve the quality of the manuscript. Regarding the general comment whether another quantity is more suitable to act as indicator for chlorine activation, temperature thresholds are adequate proxies for chlorine activation since PSC formation and chlorine activation depend primarily on the ambient temperature. Since we still don't have a complete understanding of PSC formation and therefore cannot precisely predict or model the prevailing surface area densities in the polar vortex, any quantity we could suggest to serve as an indicator for chlorine activation would also have its limitations. However, the event studied in this study is not unique nor rare. CALIOP regularly shows that optically thick PSCs tend to form over specific regions (East Greenland, Scandinavian Alps, Antarctic Peninsula). Temperature thresholds are unlikely to capture chlorine on such small scales. This is something that needs to be kept in mind when such proxies are used.

Please find below our response to all your comments.

P. 33732, L. 10/13: Please introduce HCl (hydrochloric acid) and ClONO2 (chlorine nitrate)
added hydrochloric acid and chlorine nitrate respectively when the species names where first used

P. 33732, L. 16: PSC - PSCs
changed

P. 33732, L. 19: PSCs - PSC particles
changed

P. 33732, L. 20: PSCs - PSC formation
changed

P. 33732, L. 21: PSC surface area density
changed

P. 33732, L. 24: the ozone hole → the Antarctic ozone hole
changed

P. 33733, L. 4: I think in the introductory section this should be a bit more detailed. I suggest: ... of the polar stratosphere: On the one hand heterogeneous chemistry on PSC particles impacts the partitioning of inorganic chlorine by chlorine activation, i.e. by converting inorganic chlorine reservoir species (mainly HCl and ClONO2) to photo- active species (ClOx = ClO + 2 Cl2O2). On the other hand PSC particles can grow large enough to effectively ...
changed

P. 33733, L.11: Actually, two questions are asked here and not one. I suggest:Two of the key questions are: (1) To which extent is heterogeneous chemistry on PSC particles responsible for chlorine activation and (2) what are the time-scales for this processing. Furthermore I suggest that the questions are picked up in the conclusion.
changed and the questions are now picked up again in the conclusions

P. 33733, L.14: If I understand correctly the influence of PSCs is compared to the influence of binary aerosol. I suggest: .. that the influence of PSCs on chlorine activation in subordinate to that of cold binary aerosol ..
changed

I recommend to re-organize parts of this section a little bit:
P. 33734, L.10-11: Details about the CALOP PSC classification algorithm can be found in Pitts et al. (2009, 2011, 2013). (1)
P. 33735, L.11-15: The CALIOP PSC classification .. (2)
P. 33735, L.21-25: PSCs are identified ... (3)
This paragraph gives additional information about the detection algorithm. Therefore, I think that it would better fit in the first paragraph of the section. → I suggest re-organizing it from (1)-(2)-(3) to (2)-(3)-(1).
The section has been rearranged accordingly

P. 33734, L.13: I suggest: Mixtures of STS and NAT are further divided into three groups, MIX 1, MIX 2 and MIX 2 enhanced, where NAT number density ...
changed

P. 33734, L.26: native → original
changed

P. 33735, L.6: NAT is already explained → ..(NAT existence temperature)..
removed

P. 33735, L.6ff: How large is the difference between TNAT and TACl? Values?
Both values lie generally within 2K. Drdla and Müller (2012) give a detailed comparison of both values

P. 33735, L.26: I suggest: a realistic → the
rephrased

P. 33735/6, L27-L.2: .. a relationship of what? I suggest: .. to derive a relationship between CALIOP measurements of particulate backscatter at 532 nm and the liquid particle SAD.
changed

P. 33736, L. 18: Which season? And are the used values of the parameters representative for this season?
Clarified that he used values are representative for a wide range of possible conditions in the polar vortex

P. 33736 Eq 1: I suggest writing the parentheses as in Fig. 1 b
Parentheses have been changed to agree with Fig. 1b

P. 33737, L. 7-9: The information about the temporal evolution can not be found in Fig. 2, right? Please make this clear in the text.

While Figure 2 is only a snapshot, the temporal evolution of PSC particles follows the composition of the entire PSC. This has been clarified in the text

P. 33737, L. 22: I suggest: .. processing with low values of HCl indicating air masses where ...
changed

P. 33738, L. 6: Model calculations indicate .. Does this refer to current knowledge or are the model calculations the simulations used in this study?
The calculations have been performed in this study but are not shown, this is now indicated in the manuscript

P. 33738, L. 10: .. in regions, where our calculations indicate that only unprocessed air is present, could originate ..
changed

P. 33738, L. 15-25: This paragraph I find hard to follow. It would be helpful if you indicate the Figure where to look at, e.g. in line 17. Furthermore I was wondering why it is pointed to Fig 3c to show the higher HCl mixing ratios of air that was not exposed to PSCs. I think this is also shown on the other days and not exclusively on 2 January. I suggest including e.g. . In line 24-25: After 3 January .. Is this related to the sentence before? This is a bit confusing.
Added indicators to clarify where in the figure the text refers to. Lines 24-25 have also been clarified, this sentence refers to the air which has been exposed to PSCs on 31 December.

P. 33738, L. 26: ... for air masses to circumnavigate ..
changed

P. 33739, L. 2: Vortex-averaged values .. of what? HCl?
Vortex-averaged HCl mixing ratios, clarified in the text

P. 33739, L. 10: I suggest: .. indicate the formation of STS. Figure 4d suggests ..
split into two sentences

P. 33739, L. 16: Please add the Figure number to look at.
This is visible by the white contours in each panel, clarified in the text

P. 33739, L. 16-19: As the threshold ... decreases, .. When I first read this sentence, I understood this as a temporal evolution. I suggest: With smaller threshold backscatter values chosen for the area describing the processing reactor (Fig.4d to 4a), ...
changed

P. 33741, L. 19 ff: Please add the Figure numbers to look at.
added figure references

P. 33742, L. 12: I suggest: .. as described in this study chlorine activation

on PSCs is faster than on the background aerosol.
changed

P. 33742, L. 14/15: .. the latest.. ?
removed the latest

P. 33742, L. 27: 24h → 24 hours
changed

P. 33742, L. 3: .. and allow to distinguish between ..
changed

P. 33743, L. 4-5: I suggest: The average daily HCl mixing ratio shows substantially smaller HCl values in processed than in unprocessed air.
changed

P. 33743, L. 5-6: We've shown → We show
changed

P. 33743, L. 6: a uniform → an uniform
a uniform is the correct grammar since the u in uniform is pronounced like a y.

P. 33743, L. 15: excellent → good
changed

P. 33743, L. 23-25: This sentence suggests that only ice PSCs can serve as processing reactor. Is this meant?
Changed to optically thick PSCs since SAD is the decisive factor and not PSC type.

Figures:
Figure 1: Please add the notice to the figure caption that the x-axis for SAD is on the top.
added

Figure 3: Caption: L. 1: I suggest: The meteorological situation over a six-day period from 31st December 2009 to 5th January 2010 .. L. 4: .. regions of the vortex with air which has passed through a PSC. L. 6: .. values are indicative ..
all changed

Figure 4: Please add y-labels. Furthermore, it would be interesting to know the used temperature thresholds.
y-label added. The used temperature thresholds are TNAT and TACl, both have been added to the caption.

Figure 5: Which backscatter threshold is used here for detecting processed and unprocessed air?

$3*10^{-5}km^{-1}sr^{-1}$ **has been used as threshold, added this to the caption**

Figure 6: I really had problems to understand this figure. What means the date in the title of the subfigures? Is it the initialization date of the respective trajectory? I suggest adding Trajectory 1, etc. and clarifying this is the caption. Please add a), b) .. to the figure caption.
The date refers to the day the respective trajectory encountered its maximum in backscatter. All trajectories were initialized at the same time. This has been clarified in the caption. Panel identifiers have also been added to the caption

The unit of SAD is not correct.
corrected

Vortex-wide chlorine activation by a mesoscale PSC event in the Arctic winter of 2009/10

T. Wegner[1], **M. C. Pitts**[1], **L. R. Poole**[2], **I. Tritscher**[3], **J.-U. Grooß**[3], **and H. Nakajima**[4]

[1]Chemistry and Dynamics Branch - Langley Research Center, National Aeronautics and Space Administration, Hampton, Virginia, USA
[2]Science Systems and Applications, Hampton, Virginia, USA
[3]Institute for Energy and Climate Research IEK-7, Forschungszentrum Jülich, Jülich, Germany
[4]National Institute for Environmental Studies, Tsukuba, 305-8506, Japan

Abstract. In the Arctic polar vortex of the 2009/10 winter temperatures were low enough to allow widespread formation of Polar Stratospheric Clouds (PSC). These clouds occurred during the initial chlorine activation phase which provided the opportunity to investigate the impact of PSCs on chlorine activation. Satellite observations of gas-phase species and PSCs are used in combination with trajectory modeling to assess this initial activation. The initial activation occurred in association with the formation of PSCs over the east coast of Greenland at the beginning of January 2010. Although this area of PSCs covered only a small portion of the vortex, it was responsible for almost the entire initial activation of chlorine vortex wide. Observations show HCl **(hydrochloric acid)** mixing ratios decreased rapidly in and downstream of this region. Trajectory calculations and simplified heterogeneous chemistry modeling confirmed that the initial chlorine activation continued until ClONO$_2$ **(chlorine nitrate)** was completely depleted and the activated air masses were advected throughout the polar vortex. For the calculation of heterogeneous reaction rates, surface area density is estimated from backscatter observations. Modeled heterogeneous reaction rates along trajectories intersecting with the PSC**s** indicate that the initial phase of chlorine activation occurred in just a few hours. These calculations also indicate that chlorine activation on the binary background aerosol is significantly slower than on the PSC **particles** and the observed chlorine activation can only be explained by an increase in surface area density due to PSC **formation**. Furthermore, there is a strong correlation between the magnitude of the observed HCl depletion and PSC surface area **density**.

1 Introduction

Heterogeneous chemistry on stratospheric aerosol and Polar Stratospheric Clouds (PSCs) plays a crucial role in the formation of the **Antarctic** ozone hole (Solomon, 1999). While the stratospheric aerosol layer is present globally at all times (Junge et al., 1961), PSCs only form over the polar regions of the winter hemisphere (Lowe and MacKenzie, 2008). PSCs are ubiquitous in the Antarctic winter but wide-spread PSC occurrence over the Arctic is only observed during very cold winters (Pitts et al., 2009, 2011). PSCs have a substantial influence on the chemical composition of the polar stratosphere**: On the one hand heterogeneous chemistry on PSC particles impacts the partitioning of inorganic chlorine by chlorine activation (Solomon et al., 1986), i.e. by converting inorganic chlorine reservoir species (mainly HCl and ClONO$_2$) to photo-active species (ClOx = ClO + 2*Cl$_2$O$_2$). On the other hand PSC particles can grow large enough to effectively denitrify (Fahey et al., 2001) and dehydrate (Kelly et al., 1989) the lower stratosphere.** Although PSCs have a pivotal role in determining stratospheric chemical composition and have been subject to extensive research since the 1980s, some details are still subject to uncertainty.

Two of the key questions are: (1) To which extent is heterogeneous chemistry on PSC particles responsible for chlorine activation and (2) what are the time-scales for this processing. Several studies (e.g. Drdla and Müller, 2012; Wohltmann et al., 2013; Kirner et al., 2015) have suggested **that the influence of PSCs on chlorine activation in subordinate to that of cold binary aerosol** on a vortex-wide scale. When temperatures approach the frost point, heterogeneous reaction rates are large enough to activate chlorine on time-scales of minutes to hours regardless of surface type (Wegner et al., 2012). On the other hand, Carslaw et al. (1998) and Kühl et al. (2004) showed that nearly complete chlorine activation can be achieved in a mountain-wave PSC

Correspondence to: M. Pitts
(michael.c.pitts@nasa.gov)

at sufficiently low temperatures and large surface area densities.

This study investigates the influence of mesoscale PSCs on the chemical composition of the entire vortex. Mesoscale PSCs are larger in spatial scale than mountain-wave induced PSCs but still only cover a small fraction of the polar vortex. We use data from the **Cloud-Aerosol LIdar with Orthogonal Polarization (CALIOP, Winker et al., 2009)** instrument for studying PSCs and data from the Microwave Limb Sounder **(MLS, Waters et al., 2006) in combination with model calculations of the Chemical Lagrangian Model of the Stratosphere (CLaMS, McKenna et al., 2002)** to examine the impact of a mesoscale PSC on the chemical composition of the Arctic vortex in January 2010. CALIOP backscatter observations are used to derive particle surface area density (SAD) which is then used to calculate chlorine activation. Through these analyses, we will examine the impact of PSC SAD enhancements on chlorine activation compared with the cold binary background aerosol.

2   Instrumentation and Model Description

The **Cloud-Aerosol Lidar and Infrared Pathfinder Spaceborne Observations (CALIPSO)** satellite is member of the A-train satellite constellation (Stephens et al., 2002) orbiting at an inclination of $98.2°$ that provides coverage up to $82°$ latitude in each hemisphere. Its primary instrument is CALIOP which measures backscatter at 1064 nm and 532 nm, with the 532 nm channel separated into orthogonal polarization components parallel and perpendicular to the polarization plane of the outgoing laser beam (Winker et al., 2009). **The CALIOP classification scheme distinguishes between Supercooled Ternary Solutions (STS), mixtures of STS and Nitric Acid Trihydrate (NAT) and ice. Mixtures of STS and NAT are further divided into three groups, MIX 1, MIX 2 and MIX 2 enhanced, in order of increasing NAT number density. CALIOP also distinguishes between synoptic and wave ice. PSCs are identified in the CALIOP measurements as enhancements in backscatter at 532 nm with an altitude dependent threshold of β_{532} between 2 and $4 \cdot 10^{-5} km^{-1} sr^{-1}$ in the algorithm described in Pitts et al. (2013). We show sensitivity studies that use different threshold backscatter ratios between $3 \cdot 10^{-5} km^{-1} sr^{-1}$ and $1.5 \cdot 10^{-4} km^{-1} sr^{-1}$, where the latter backscatter threshold is high enough to indicate the presence of ice PSCs. Details about the CALIOP PSC classification algorithm can be found in Pitts et al. (2009, 2011, 2013).**

The Microwave Limb Sounder (MLS) is an instrument on the Aura satellite, which is also part of the A-train constellation and has provided nearly continuous measurements since 2004 (Waters et al., 2006). MLS provides about 3500 profiles of gas-phase species and temperature from Earth's surface to 90 km altitude between 82°N and 82°S per day. In this study, we use MLS HCl data from retrieval version 3.3 (Livesey et al., 2011) which is comparable to version 2.2. Retrieval version 2.2 for HCl has been validated in Santee et al. (2008). The vertical resolution and precision of the HCl observations are 3 km and 0.2-0.3 ppbv, respectively.

CALIOP and MLS observations are linearly interpolated to a $20°$ by $2°$ (longitude x latitude) grid on fixed potential temperature surfaces each day. Potential temperature is calculated from the **original** MLS pressure levels and temperature data from the Modern-Era Retrospective Analysis for Research and Applications (MERRA, Rienecker et al., 2011).

Air mass trajectories are calculated with CLaMS which uses a fourth-order Runge-Kutta scheme. The wind fields for these trajectories are taken from ERA-INTERIM (Dee et al., 2011). Threshold temperatures T_{NAT} (NAT existence temperature) and T_{ACl} (chlorine activation temperature) which can serve as indicators for chlorine activation (Drdla and Müller, 2012) are calculated with temperatures and trace gas concentration from a CLaMS simulation described in Grooß et al. (2014). The vortex edge is defined according to Nash et al. (1996).

A simple algorithm was defined to determine the locations of air masses that had previously passed through the PSC event. Trajectories are used to track air masses downwind of a PSC that is defined by the CALIOP detection threshold. These air masses are called "Processed Air" since we assume that chlorine activation predominantly occurred in such air masses. On a given day a grid box is labeled as filled with "Processed Air" if a processed air mass has passed through this grid box on that day. A grid box is then labeled as filled with "Unprocessed Air" if on a given day no processed air masses have passed through this grid box even if this grid box was marked with "Processed Air" on previous days. This way we can describe for each day the fraction of the vortex that is filled with air masses which have previously encountered a PSC.

The determination of heterogeneous reaction rates requires an estimation of the particle surface area density (SAD) of PSCs and the background aerosol as realistic as possible. Following the approach of Gobbi (1995), we performed Mie calculations for unimodal lognormal particle size distributions representative of the polar stratosphere to derive a relationship **between CALIOP measurements of particulate backscatter at 532 nm and the liquid particle SAD.** Figure 1a shows calculated liquid particle SAD and backscatter ($\beta_{532,\text{liquid}}$) as a function of temperature relative to the frost point (T-T$_{\text{frost}}$) for the following conditions: pressure = 30 hPa, HNO$_3$ = 15 ppbv, H$_2$O = 5 ppmv, particle number density N = 10 cm^{-3} (Curtius et al., 2005), and lognormal geometric standard deviation σ = 1.6 (Lambert et al., 2012). For these calculations, liquid particle volume was prescribed as a function of temperature according to Carslaw et al. (1995); mode radius (for the Mie calcula-

tions) and SAD were then calculated from particle volume using standard relationships for a unimodal lognormal.

Calculated values of liquid SAD and $\beta_{532,\mathrm{liquid}}$ from Figure 1a are plotted against each other in Figure 1b. The dashed curve shows the least-squares quadratic fit in log-log space between the two parameters, which we will use in this study. With fixed N = 10 cm^{-3} and σ = 1.6, **calculated** points fall along the same least-squares curve for different pressure levels (50 and 70 hPa), HNO$_3$ mixing ratios (2, 5, and 10 ppbv), and H$_2$O mixing ratio (2 ppmv). Values **calculated** for different values of N (5 and 15 cm^{-3}) and σ (1.3 and 1.8) fall along different curves, but all points lie within the limits depicted by the solid gray curves. Given the small envelope defined by those parameters the relationship between SAD and $\beta_{532,\mathrm{liquid}}$ is robust and **covers a wide range of possible conditions in the polar vortex.** Measured values of $\beta_{532,\mathrm{liquid}}$ larger than **1.5·10^{-4}** $km^{-1}sr^{-1}$ likely signify ice PSCs. The SAD estimated using the least-squares relationship for liquid particles can be considered a lower limit of SAD for ice PSCs. The relationship between backscatter and surface area density for STS particles can then be described by:

$$log_{10}SAD = 3.474 + 0.671 \cdot log_{10}\beta_{532} + 0.007 \cdot *log_{10}\beta_{532})^2 \quad (1)$$

Fig. 1. a) Temperature dependence of STS surface area density **(top x-scale)** and the corresponding theoretical backscatter signal at 532 nm for typical stratospheric conditions. b) Relationship between STS surface area density and particulate backscatter color coded according to their theoretical temperature. Gray curves mark the deviation from the fitted function for varying ambient conditions.

3 The Mesoscale PSC Event

Near the end of December 2009, CALIOP observed an increase in backscatter over Greenland, corresponding to the first major formation of liquid **and** ice PSCs (Pitts et al., 2011) during the Arctic winter 2009/10. The increase in SAD indicates condensation of HNO$_3$ on the background aerosol or the nucleation of NAT and ice particles. The PSC backscatter and areal extent increased during the following two days reaching a maximum on 2 January 2010 before slowly decreasing on subsequent days. Figure 2 shows the PSC classification according to Pitts et al. (2011) from the CALIOP observations on 2 January. The PSC extends between 20-25 km in altitude and is a mixture of all PSC types. CALIOP observations indicate that STS forms first over the west coast of Greenland followed by wave ice formation over central Greenland. Synoptic ice and NAT mixtures occur downstream of the wave ice over eastern Greenland. **While Figure 2 represents only a snapshot of the PSC, it also provides information about the temporal evolution of PSC particles. The temporal evolution of PSC particles within a confined air mass will look very similar to the geographical distribution depicted in Figure 2, with STS forming first, followed by ice and NAT particles.** Figure 2 also shows the limitations of our current observations with gaps of hundreds of kilometers between the orbits. During this PSC event, the vortex was shifted away from the pole over northeast Canada and northern Russia. The vor-
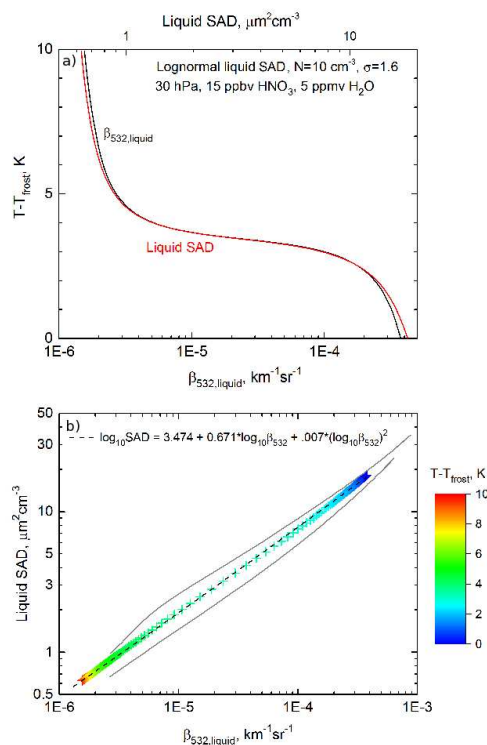
tex remained stable during this time-frame with only limited dynamic disturbances.

Figure 3 shows backscatter over a six-day period from 31 December 2009 to 5 January 2010 and the prevailing winds. From the meteorological data we estimate the wind speed in the vicinity of the PSC to be 20 m/s which yields a residence time of about one day for air parcels traveling through the PSC. Chlorine activation is limited by the availability of the reservoir species and will cease once either HCl or ClONO$_2$ are depleted (Portmann et al., 1996). Heterogeneous chemistry on stratospheric aerosols is primarily the conversion of HCl and ClONO$_2$ into ClO$_x$ (ClO + 2·Cl$_2$O$_2$). Therefore, the observations of gas-phase HCl by MLS can serve as an indicator of heterogeneous **processing with low values of HCl indicating air masses where** inorganic chlorine has been activated. Since HCl is more abundant than ClONO$_2$ at the beginning of winter, ClONO$_2$ is the limiting component in chlorine activation (Portmann et al., 1996).
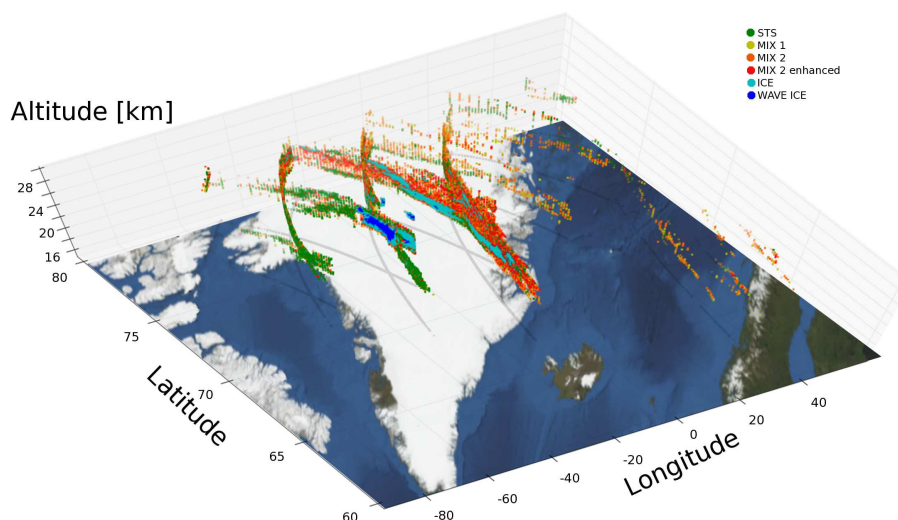
Fig. 2. CALIOP PSC observations along orbits over Greenland on 2 January 2010 color coded according to the CALIOP classification. Green: STS; Yellow: MIX 1; Orange: MIX 2; Red: MIX 2 enhanced; Cyan: Synoptic Ice; Blue: Wave Ice

Figure 3a shows that low HCl mixing ratios are co-located with the PSCs over northern Greenland on 31 December and that HCl mixing ratios upstream of the PSC are more than twice as high compared to air exposed to the PSC. CALIOP observed backscatter values above $1.5 \cdot 10^{-4} km^{-1} sr^{-1}$ which corresponds to a tenfold increase of SAD relative to background conditions, or to around 10 $\mu m^2 cm^{-3}$. During all subsequent days, HCl is always lower in the vicinity of PSCs compared to areas upstream with HCl mixing ratios decreasing to less than 0.5 ppbv during this period, about a quarter of their values in a chemically unperturbed vortex.

The low HCl mixing ratios persist downstream of the PSCs and do not decrease further, in agreement with current knowledge that chlorine activation is highly dependent on SAD, temperature and the ratio of HCl/ClONO$_2$. Model calculations **(not shown)** indicate that ClONO$_2$ is totally depleted downstream of the PSC. Additional activation can only occur when ClONO$_2$ is regenerated (Portmann et al., 1996). ClONO$_2$ controls the total amount of chlorine that can be activated while PSCs determine the area in which activation occurs. Low HCl concentrations observed **in regions, where our calculations indicate that only unprocessed air is present, could originate** from either physical mixing with processed air or averaging along the MLS field of view. We also need to stress that such trajectory calculations rely on the quality of the wind fields used and are subject to errors which are difficult to quantify.

The air which was exposed to PSCs on 31 December 2009 **(Fig. 3a, enclosed by red and blue contour lines)** has completed a full circumnavigation of the vortex after five days **(5 January 2010, Fig. 3f)** and re-entered the region where it first encountered PSCs. Air which was not exposed to PSCs

tends to have higher HCl mixing ratios, indicating that little chlorine activation occurred outside of PSCs, as shown clearly**, for example, on** 2 January in Figure 3c. Air **between Norway and Novaya Zemlya** followed its own cyclonic circulation separate from the polar vortex. Air in this region did not encounter PSCs nor sunlight, leading to constant HCl mixing ratios. This situation persisted for several days and the trajectories passing through PSCs actually flowed around this region. After 3 January **(Fig. 3d-e)** air **with low HCl mixing ratios** flows into the PSC covered area from the unobserved area north of 82° so we do not have a complete history of HCl concentrations in relation to PSC exposure for these air masses.

As Figure 3 indicates, it takes about five days **for air masses to circumnavigate** the polar vortex. This means that a PSC with a sufficiently large meridional extent can activate chlorine throughout the entire vortex even when the PSC itself only covers a small fraction of the vortex. Such a PSC can serve as a "processing reactor" for chlorine activation with heterogeneous chemistry basically limited to the time air masses spend inside the PSC. Vortex-averaged **HCl mixing ratios** which are commonly used to estimate chlorine activation would not accurately represent the true nature of activation within the vortex, under these conditions.

While chlorine activation is generally observed within the boundary of elevated backscatter values as observed by CALIOP, the lowest HCl mixing ratios are correlated with the highest backscatter values. Figure 4 shows the ratio of mean HCl mixing ratios in processed air which has been exposed to backscatter values above certain thresholds to the vortex average HCl mixing ratio. The backscatter thresholds in Figure 4a-c indicate the formation of STS. **Figure** 4d
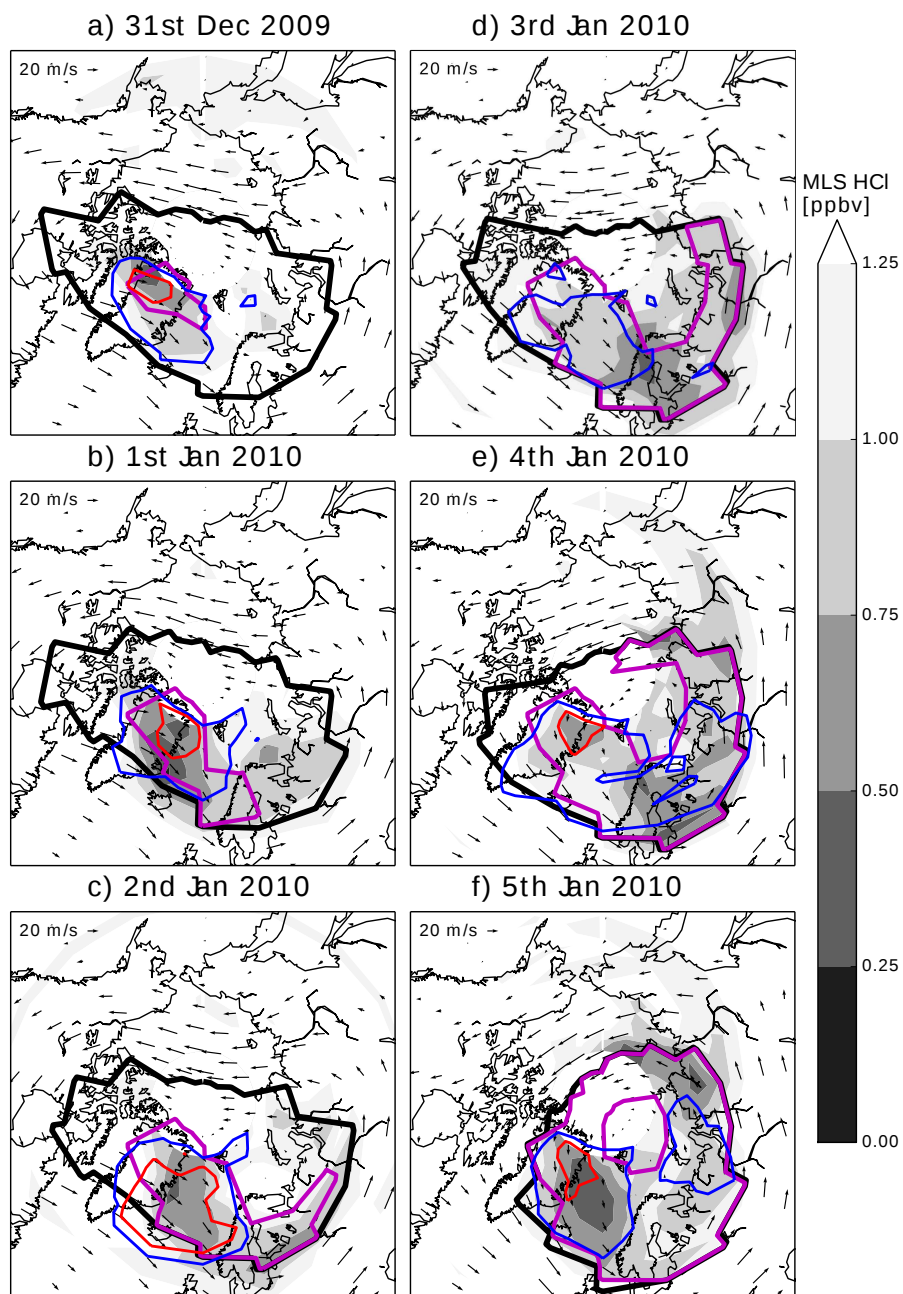
Fig. 3. The meteorological situation over a six-day period from 31 December 2009 to 5 January 2010 for the Arctic winter 2009/2010 on the 510 K isentrope (approximately 22 km). Arrows show the prevailing wind direction and speed. The vortex edge is calculated according to Nash et al. (1996) and shown in solid black. Solid magenta indicates regions of the vortex **with** air which has passed through a PSC. Blue and red contours show the particulate backscatter from CALIOP where blue represents the detection limit for CALIOP ($3 * 10^{-5} km^{-1} sr^{-1}$) and red values **are** indicative of PSCs with a surface area density of more than 10 times the background values ($1.5 * 10^{-4} km^{-1} sr^{-1}$). Grey contours show HCl mixing ratios from MLS.

suggests the presence of ice since backscatter values of this magnitude correspond to higher surface area densities than physically possible with only the condensation of HNO_3.

The ratio of mean HCl mixing ratios to the vortex aver-

age HCl mixing ratio is also shown for air which has been exposed to temperatures below either T_{NAT} or T_{ACl}. After five days the HCl mixing ratios within processed air are indistinguishable from the vortex mean **(indicated by the**

white contour on the right side of each panel) because
all air within the vortex has been exposed to PSCs. **With
smaller threshold backscatter values chosen for the area
describing the processing reactor (Fig. 4d to 4a),** HCl mix-
ing ratios in air which has been exposed to PSCs gradually
approaches the vortex average. This shows that chlorine acti-
vation occurs locally in the area covered by PSCs but not on
a vortex wide scale.

Temperature thresholds for chlorine activation do not cap-
ture this localized effect. The air exposed to an area enclosed
by a temperature threshold is always very similar to the vor-
tex average since those areas already encompass the main
part of the vortex. Therefore, neither T_{NAT} nor T_{ACl} pro-
vide realistic information on the location where chlorine ac-
tivation occurs for the period considered in this study. Only
thresholds based on backscatter provide this information.

In addition, Figure 4 indicates that at the beginning of the
activation phase under study, the average HCl mixing ratio
in the area above a chosen backscatter threshold decreases
as the backscatter threshold is increased. Since backscatter
can be used as a proxy for surface area density, the surface
area provided by PSCs appears to have a direct affect on gas-
phase HCl concentrations. While HCl mixing ratios above
a backscatter threshold indicative of STS (Figure 4a) have a
minimum of 70% of vortex average HCl mixing ratios, HCl
mixing ratios above a threshold suggestive of ice PSCs (Fig-
ure 4d) have a minimum of 50% of the vortex average HCl
mixing ratios. Therefore, chlorine activation processes vis-
ibly faster with increasing surface area density. The mag-
nitude of chlorine activation appears to be correlated with
available surface area density provided by PSCs.

The mesoscale PSC event leaves a visible mark on HCl
mixing ratios. When separating the polar vortex into regions
of processed and unprocessed air, we find lower HCl mix-
ing ratios in processed air (Figure 5) between 31 December
and 9 January. Observations by MLS show that for all days
between 20-25 km, HCl is lower in processed air compared
to unprocessed air. However, the large uncertainties indicate
that the distinction between processed and unprocessed air is
difficult and that the mean values are calculated from hetero-
geneous air masses. Still, we see a clear trend that chlorine
activation has progressed further in air masses which have
been exposed to PSCs.

The analysis for Figure 5 was repeated with T_{NAT} and
T_{ACl} (not shown) as indicators for processed air. Here, pro-
cessed air describes those grid boxes with temperatures less
than the respective threshold temperatures and grid boxes
where trajectories are present which have encountered tem-
peratures less than the temperature thresholds in their past.
Two main differences emerge. First, the daily mean mixing
ratios for processed and unprocessed air are more similar,
making a distinction between them difficult. Second, pro-
cessed air covers the entire vortex more quickly because both
temperature thresholds cover a larger area of the vortex than
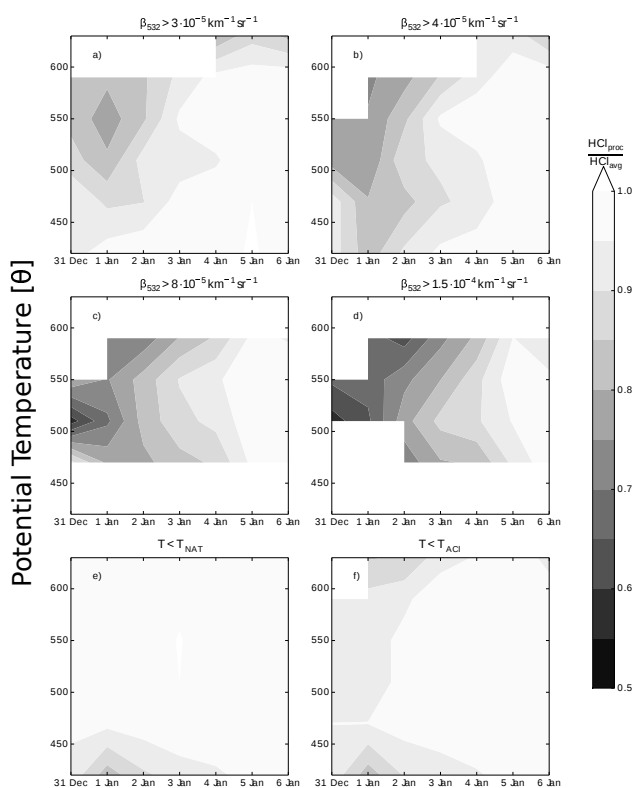our PSC threshold. This leads to fewer available data points.

Fig. 4. Ratio of average HCl mixing ratio of air that passed through
a specified area to the vortex average HCl mixing ratio. The ratio is
calculated for six areas, four encompassed by backscatter thresholds
(a)-d)) and two by temperature thresholds (**T_{NAT}, e)** and **T_{ACl}, f)**).
A ratio of less than one indicates air inside the contour has a lower
HCl mixing ratio than the vortex average.

Using either of the temperature thresholds to describe pro-
cessed air does not show any significant difference between
processed and unprocessed air.

4   Modeling heterogeneous chemistry

For a quantitative understanding of the shown HCl decrease
we use the trajectories combined with a very simplified het-
erogeneous chemistry scheme. Using the relationship in
Equation 1, we can use CALIOP backscatter to calculate
PSC SAD along trajectories passing through the maximum
PSC backscatter. The trajectories are initialized with H_2O,
HNO_3 and HCl from MLS observations and it is assumed
that at the start of the trajectories no chlorine has been ac-
tivated yet. Hence, $ClONO_2$ is initialized as the difference
between total inorganic chlorine (Cl_y) and HCl with Cl_y
derived from the Cl_y-N_2O tracer-tracer relationship (Grooß
et al., 2002). The simplified chemistry consists of three het-
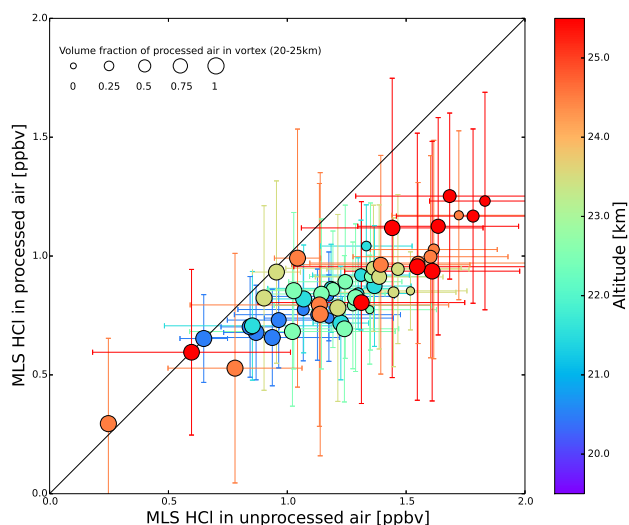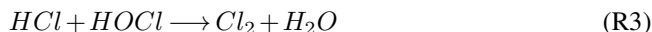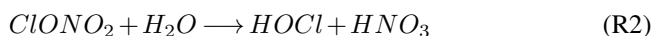erogeneous reactions which are modeled along the trajecto-

Fig. 5. Correlation of daily average MLS HCl in processed (**Backscatter threshold:** $3 * 10^{-5} km^{-1} sr^{-1}$) and unprocessed air from 12/31 to 01/09 for six different altitudes. Error bars indicate the 1-σ standard deviation of calculating the daily average HCl mixing ratios.

ries:

$$HCl + ClONO_2 \longrightarrow Cl_2 + HNO_3 \qquad (R1)$$

$$ClONO_2 + H_2O \longrightarrow HOCl + HNO_3 \qquad (R2)$$

$$HCl + HOCl \longrightarrow Cl_2 + H_2O \qquad (R3)$$

No additional reactions are included in the calculations since they are not relevant to assess chlorine activation on time-scales of up to one day. The uptake coefficients for all three reactions are calculated for STS even when backscatter values indicate the presence of ice. However, no difference in HCl mixing ratios is evident when the uptake coefficients for ice are used once backscatter values suggest the presence of ice PSCs.

Figure 6**a-c** shows three trajectories which encounter their backscatter maximum on three different days. The maximum backscatter suggests the presence of ice clouds on 1,2 and 3 January **for all three trajectories**; however, temperatures only decrease below the frost point on 6 January for **trajectory 1 which encountered its backscatter maximum on 31 December (Fig. 6a.)**

The evolution of modeled HCl and observations (**Fig. 6d-f**) shows very good agreement for the first activation phase. **Nakajima et al. (2015) also reported very good agreement of model and observations during this phase.** HCl along the trajectories deviates from the observations after a couple of days. However, chlorine activation in the first half of the trajectories can still be analyzed. A decrease in HCl coincides with an increase in surface area density and ClONO_2 is

totally depleted after the initial activation. This confirms that ClONO_2 is indeed the limiting factor for chlorine activation because observed HCl also does not decrease further once the model shows complete removal of ClONO_2. The complete removal of ClONO_2 also occurs before the maximum in surface area density (**Fig. 6d-f**) but activation starts when SAD increases above background values. Neither observations nor modeled chemistry indicate significant chlorine activation in the absence of PSCs. In fact, when heterogeneous chemistry is only modeled on a binary sulfate aerosol (without uptake of HNO_3 as temperatures decrease) chlorine activation does not only progress slower (Figure 6d-f) dashed lines) but also does not completely deplete ClONO_2.

While previous studies have shown that for an entire winter season heterogeneous chemistry on cold binary aerosol is sufficient to achieve complete chlorine activation (Drdla and Müller, 2012; Wohltmann et al., 2013), in the case of a mesoscale event **as described in this study chlorine activation on PSCs is faster than on the background aerosol.** The observed activation could not have occurred without the additional surface area provided by PSCs. However, Figure 6f also shows that after five days, heterogeneous chemistry on only the binary aerosol has depleted all the initially available ClONO_2. In agreement with Drdla and Müller (2012) the degree of chlorine activation on only the background aerosol would become indistinguishable from chlorine activation on PSCs after about 10 days, or the time it takes for an air parcel to fully circumnavigate the vortex twice.

5 Conclusions

We have analyzed CALIOP and MLS observations in combination with modeled trajectories to quantify the initial chlorine activation phase for the winter 2009/10 and constrain the spatial and temporal scales on which chlorine activation occurred**; thus, answer the questions of the extent to which heterogeneous chemistry on PSC particles is responsible for chlorine activation and the time-scales for this processing.** Our analysis has shown that mesoscale PSCs can have a substantial effect on chlorine chemistry throughout the polar vortex, even though the PSCs themselves only cover a small fraction of the polar vortex. A substantial decrease in HCl is observed in air masses exposed to PSCs for about 24 **hours**. MLS observations indicate that air masses with low HCl mixing ratios occur downstream of this PSC event in agreement with the trajectory calculations. The modeled trajectories provide a solid approximation of the path the air has taken after it encountered the PSC and **allow to** distinguish between processed and unprocessed air masses. **The average daily HCl mixing ratio shows substantially smaller HCl values in processed than in unprocessed air. We** also show that chlorine activation in the polar vortex is not always a uniform process but can occur in mesoscale PSC "processing reactors". Heterogeneous chemistry occurs in
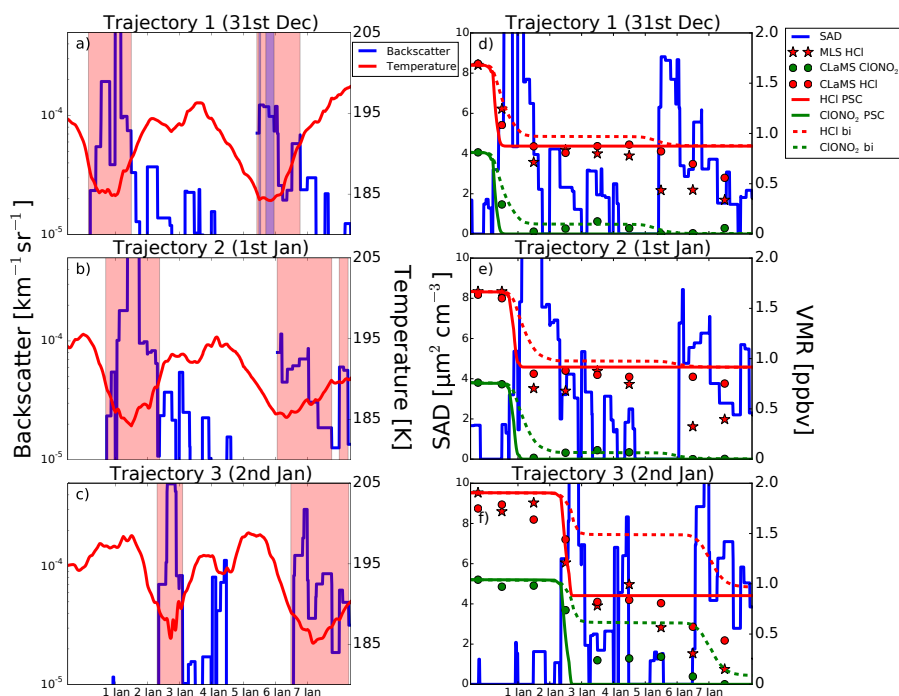
Fig. 6. Temporal evolution of **three** trajectories on 510 K potential temperature **which encounter their** backscatter maximum on three different days. **Trajectories were initialized at the same time and the period from 30 December 2009 to 8 January 2010 is shown for all three.** Left column **(a-c)** shows backscatter (blue), temperature (red), time below T_{NAT}-3K (red shading) and time below T_{ICE} (blue shading) **for the trajectories**. Right column **(d-f)** shows surface area density (blue), HCl (red) and ClONO$_2$ (green). Red stars are the daily mean HCl mixing ratios observed by MLS interpolated on the position of the trajectory and circles are CLaMS mixing ratios of HCl (red) and ClONO$_2$ (green), respectively. Solid red and green lines represent HCl and ClONO$_2$ where SAD for calculating heterogeneous reaction rates is calculated from the observed backscatter. Dashed red and green lines represent HCl and ClONO$_2$ where SAD is calculated for a binary aerosol.

these "processing reactors" and the air is subsequently advected and mixed throughout the vortex. Chlorine activation does not occur homogeneously throughout the vortex and HCl mixing ratios can vary significantly, especially during this initial activation phase. Therefore, a vortex average point of view does not provide an accurate representation during this phase. The trajectory calculations show that the availability of ClONO$_2$ limits the extent of chlorine activation. For the first time, CALIOP backscatter observations were utilized to estimate surface area density and model heterogeneous chemistry along trajectories. Results from these simulations are in **good** agreement with observed mixing ratios of HCl. These calculations also show that the SAD enhancements from PSCs lead to faster chlorine activation than would occur on the background aerosol. While the background aerosol could eventually activate the same amount of chlorine as the PSCs, over the time and spatial scales considered in this study, the observed rate of chlorine activation can only be explained by the additional surface area provided by PSCs. While this study focuses on the Arctic, similar conditions like the situation over Greenland in January 2010 can

also occur over the Antarctic. **Optically thick PSCs** over Antarctica predominantly occur over the Antarctic peninsula; therefore, this area can also serve as a processing reactor for chlorine activation.

References

Carslaw, K. S., Luo, B., and Peter, T.: An analytic expression for the composition of aqueous HNO$_3$-H$_2$SO$_4$ stratospheric aerosols including gas phase removal of HNO$_3$, Geophys. Res. Lett., 22, 1887–1880, 1995.

Carslaw, K. S., Wirth, M., Luo, B. P., Dörnbrack, A., Leutbecher, M., Volkert, H., nad J. T. Bacmeister, W. R., Reimer, E., and Peter, T.: Increased stratospheric ozone depletion due to mountain-induced atmospheric waves, Nature, 391, 675–678, doi:10.1038/35589, 1998.

Curtius, J., Weigel, R., Vössing, H.-J., Wernli, H., Werner, A., Volk, C.-M., Konopka, P., Krebsbach, M., Schiller, C., Roiger, A., Schlager, H., Dreiling, V., and Borrmann, S.: Observations of meteoric material and implications for aerosol nucleation in the winter Arctic lower stratosphere derived from in situ particle measurements, Atmos. Chem. Phys., 5, 3053–3069, doi:10.5194/acp-5-3053-2005, 2005.

Dee, D. P., Uppala, S. M., Simmons, A. J., Berrisford, P., Poli, P., Kobayashi, S., Andrae, U., Balmaseda, M. A., Balsamo, G., Bauer, P., Bechtold, P., Beljaars, A. C. M., van de Berg, L., Bidlot, J., Bormann, N., Delsol, C., Dragani, R., Fuentes, M., Geer, A. J., Haimberger, L., Healy, S. B., Hersbach, H., Hólm, E. V., Isaksen, L., Kållberg, P., Köhler, M., Matricardi, M., McNally, A. P., Monge-Sanz, B. M., Morcrette, J.-J., Park, B.-K., Peubey, C., de Rosnay, P., Tavolato, C., Thépaut, J.-N., and Vitart, F.: The ERA-Interim reanalysis: configuration and performance of the data assimilation system, Q.J.R. Meteorol. Soc., 137, 553–597, doi:10.1002/qj.828, 2011.

Drdla, K. and Müller, R.: Temperature thresholds for chlorine activation and ozone loss in the polar stratosphere, Ann. Geophys., 30, 1055–1073, doi:10.5194/angeo-30-1055-2012, 2012.

Fahey, D. W., Gao, R. S., Carslaw, K. S., Kettleborough, J., Popp, P. J., Northway, M. J., Holecek, J. C., Ciciora, S. C., McLaughlin, R. J., Thompson, T. L., Winkler, R. H., Baumgardner, D. G., Gandrud, B., Wennberg, R. O., Dhaniyala, S., McKinney, K., Peter, T., Salawitch, R. J., Bui, T. P., Elkins, J. W., Webster, C. R., Atlas, E. L., Jost, H., Wilson, J. C., Herman, R. L., Kleinböhl, A., and von König, M.: The detection of large HNO$_3$-containing particles in the winter Arctic stratosphere, Science, 291, 1026–1031, doi:10.1126/science.1057265, 2001.

Gobbi, G. P.: Lidar estimation of stratospheric aerosol properties: Surface, volume and extinction to backscatter ratio, J. Geophys. Res., 100, 11 219–11 235, doi:10.1029/94JD03106, 1995.

Grooß, J.-U., Günther, G., Konopka, P., Müller, R., McKenna, D. S., Stroh, F., Vogel, B., Engel, A., Müller, M., Hoppel, K., Bevilacqua, R., Richard, E. an Webster, C. R., J. W. Elkins, Hurst, D. F., Romashkin, P. A., and Baumgardner, D. G.: Simulation of ozone depletion in spring 2000 with the Chemical Lagrangian Model of the Stratosphere (CLaMS), J. Geophys. Res., 107, 8295, doi:10.1029/2001JD000456, 2002.

Grooß, J.-U., Engel, I., Borrmann, S., Frey, W., Günther, G., Hoyle, C. R., Kivi, R., Luo, B. P., Molleker, S., Peter, T., Pitts, M. C., Schlager, H., Stiller, G., Vömel, H., Walker, K. A., and Müller, R.: Nitric acid trihydrate nucleation and denitrification in the Arctic stratosphere, Atmospheric Chemistry and Physics, 14, 1055–1073, doi:10.5194/acp-14-1055-2014, 2014.

Junge, C. E., Chagnon, C. W., and Manson, J. E.: Stratospheric aerosols, Journal of Meteorology, 18, 81–108, 1961.

Kelly, K. K., Tuck, A. F., Murphy, D. M., Proffitt, M. H., Fahey, D. W., Jones, R. L., McKenna, D. S., Loewenstein, M., Podolske, J. R., Strahan, S. E., Ferry, G. V., Chan, K. R., Vedder, J. F., Gregory, G. L., Hypes, W. D., McCormick, M. P., Browell, E. V., and Heidt, L. E.: Dehydration In The Lower Antarctic Stratosphere During Late Winter And Early Spring, 1987, J. Geophys. Res., 94, 11 317–11 357, doi:10.1029/JD094iD09p11317, 1989.

Kirner, O., Müller, R., Ruhnke, R., and Fischer, H.: Contribution of liquid, NAT and ice particles to chlorine activation and ozone depletion during Antarctic winter and spring, Atmos. Chem. Phys., 15, 2019–2030, doi:10.5194/acp-15-2019-2015, 2015.

Kühl, S., Dörnbrack, A., Wilms-Grabe, W., Sinnhuber, B.-M., Platt, U., and Wagner, T.: Observational evidence of rapid chlorine activation by mountain waves above northern Scandinavia, J. Geophys. Res., 109, doi:10.1029/2004JD004797, 2004.

Lambert, A., Santee, M. L., Wu, D. L., and Chae, J. H.: A-train CALIOP and MLS observations of early winter Antarctic polar stratospheric clouds and nitric acid in 2008, Atmos. Chem. Phys., 12, 2899–2931, doi:10.5194/acp-12-2899-2012, 2012.

Livesey, N. J., Read, W. G., Froidevaux, L., Lambert, A., Manney, G. L., Pumphrey, H. C., Santee, M. L., Schwartz, M. J., Wang, S., Cofeld, R. E., Cuddy, D. T., Fuller, R. A., Jarnot, R. F., Jiang, J. H., Knosp, B. W., Stek, P. C., Wagner, P. A., and Wu., D. L.: Version 3.3 Level 2 data quality and description document, Technical Report JPL D-33509, Jet Propulsion Laboratory, 2011.

Lowe, D. and MacKenzie, A. R.: Polar stratospheric cloud microphysics and chemistry, J. Atmos. Solar-Terr. Phys., 70, 13–40, 2008.

McKenna, D. S., Konopka, P., Grooß, J.-U., Günther, G., Müller, R., Spang, R., Offermann, D., and Orsolini, Y.: A new Chemical Lagrangian Model of the Stratosphere (CLaMS): 1.Formulation of advection and mixing, J. Geophys. Res., 107, 4309, doi:10.1029/2000JD000114, 2002.

Nakajima, H., Wohltmann, I., Wegner, T., Takeda, M., Pitts, M. C., Poole, L. R., Lehmann, R., Santee, M. L., and Rex, M.: Polar Stratospheric Cloud evolution and chlorine activation measured by CALIPSO and MLS, and modelled by ATLAS, Atmos. Chem. Phys. Disc., 15, 22 141–22 182, doi:10.5194/acpd-15-22141-2015, 2015.

Nash, E. R., Newman, P. A., Rosenfield, J. E., and Schoeberl, M. R.: An objective determination of the polar vortex using Ertel's potential vorticity, J. Geophys. Res., 101, 9471–9478, 1996.

Pitts, M. C., Poole, L. R., and Thomason, L. W.: CALIPSO polar stratospheric cloud observations: second-generation detection algorithm and composition discrimination, Atmos. Chem. Phys., 9, 7577–7589, 2009.

Pitts, M. C., Poole, L. R., Dörnbrack, A., and Thomason, L. W.: The 2009-2010 Arctic polar stratospheric cloud season: a CALIPSO perspective, Atmos. Chem. Phys., 11, 2161–2177, doi:10.5194/acp-11-2161-2011, 2011.

Pitts, M. C., Poole, L. R., Lambert, A., and Thomason, L. W.: An assessment of CALIOP polar stratospheric cloud composition classification, Atmospheric Chemistry and Physics, 13, 2975–2988, doi:10.5194/acp-13-2975-2013, 2013.

Portmann, R. W., Solomon, S., Garcia, R. R., Thomason, L. W., Poole, L. R., and McCormick, M. P.: Role of aerosol variations in anthropogenic ozone depletion in the polar regions, J. Geophys. Res., 101(D17), 22 991–23 006, 1996.

Rienecker, M. M., Suarez, M. J., Gelaro, R., Todling, R., Bacmeister, J., Liu, E., Bosilovich, M. G., Schubert, S. D., Takacs,

L., Kim, G.-K., Bloom, S., Chen, J., Collins, D., Conaty, A., da Silva, A., Gu, W., Joiner, J., Koster, R. D., Lucchesi, R., Molod, A., Owens, T., Pawson, S., Pegion, P., Redder, C. R., Reichle, R., Robertson, F. R., Ruddick, A. G., Sienkiewicz, M., and Woollen, J.: MERRA: NASA's Modern-Era Retrospective Analysis for Research and Applications, J. Climate, 24, 3624–3648, doi:10.1175/JCLI-D-11-00015.1, 2011.

Santee, M. L., Lambert, A., Read, W. G., Livesey, N. J., Manney, G. L., Cofield, R. R., Cuddy, D. T., Daffer, W. H., Froidevaux, L., Fuller, R. A., Jarnot, R. F., Knosp, B. W., Perun, V. S., Snyder, W. V., Stek, P. C., Thurstans, R. P., Wagner, P. A., Waters, J. W., Connor, B., Urban, J., Murtagh, D., Ricaud, P., Barret, B., Kleinböhl, A., J, K., Küllmann, H., von Hobe, M., Toon, G. C., and Stachnik, R. A.: Validation of the Aura Microwave Limb Sounder ClO measurements, J. Geophys. Res, 113, D15S22, doi: 10.1029/2007JD008762, 2008.

Solomon, S.: Stratospheric ozone depletion, A review of concepts and history, Rev. Geophys., 37, 275–316, 1999.

Solomon, S., Garcia, R. R., Rowland, F. S., and Wuebbles, D. J.: On the depletion of Antarctic ozone, Nature, 321, 755–758, 1986.

Stephens, G. L., Vane, D., Boain, R., Mace, G., Sassen, K., Wang, Z., Illingworth, A., O'Connor, E., Rossow, W., Durden, S., Miller, S., Austin, R., Benedetti, A., Mitrescu, C., and Team, C. S.: The CloudSat mission and the A-Train: A new dimension of space-based observations of clouds and precipitation, Bull. Amer. Meteorol. Soc., 83, 1771–1790, doi: 10.1175/BAMS-83-12-1771, 2002.

Waters, J. W., Froidevaux, L., Harwood, R. S., Jarnot, R. F., Pickett, H. M., Read, W. G., Siegel, P. H., Cofield, R. R., Filipak, M. J., Flower, D. A., Holden, J. R., Lau, G. K., Livesey, N. J., Manney, G. L., Pumphrey, H. C., Santee, M. L., Wu, D. L., Cuddy, D. T., Lay, R. R., Loo, M. S., Perun, C. S., Schwartz, M. J., Stek, P. C., Thurstans, R. P., Boyles, M. A., Chandra, K. M., Chavez, M. C., Chen, G.-S., Chudasama, B. V., Dodge, R., Fuller, R. A., Girard, M. A., Jiang, J. H., Jiang, Y., Knosp, B. W., LaBelle, R. C., Lam, J. C., Lee, K. A., Miller, D., Oswald, J. E., Patel, N. C., Pukala, D. M., Quintero, O., Scaff, D. M., Snyder, W. V., Tope, M. C., Wagner, P. A., and Walch, M. J.: The Earth Observing System Microwave Limb Sounder (EOS MLS) on the Aura Satellite, IEEE Transactions on Geoscience and Remote Sensing, 44, doi:10.1109/TGRS.2006.873771, 2006.

Wegner, T., Grooß, J.-U., von Hobe, M., Stroh, F., Sumińska-Ebersoldt, O., Volk, C. M., Hösen, E., Mitev, V., Shur, G., and Müller, R.: Chlorine activation on stratospheric aerosols: Uncertainties in parameterizations and surface area, Atmos. Chem. Phys, 12, 11 095–11 106, doi:10.5194/acp-12-11095-2012, 2012.

Winker, D. M., Vaughan, M. A., Omar, A., Hu, Y., Powell, K. A., Liu, Z., Hunt, W. H., and Young, S. A.: Overview of the CALIPSO Mission and CALIOP Data Processing Algorithms, J. Atmos. Oceanic Technol., 26, 2310–2323, doi: 10.1175/2009JTECHA1281.1, 2009.

Wohltmann, I., Wegner, T., Müller, R., Lehmann, R., Rex, M., Manney, G. L., Santee, M. L., Bernath, P., Sumińska-Ebersoldt, O., Stroh, F., von Hobe, M., Volk, C. M., Hösen, E., Ravegnani, F., Ulanovsky, A., and Yushkov, V.: Uncertainties in modelling heterogeneous chemistry and Arctic ozone depletion in the winter 2009/2010, Atmospheric Chemistry and Physics, 13, 3909–3929, doi:10.5194/acp-13-3909-2013, 2013.

...